ARTICLE
Journal of Cellular Biochemistry 114:2138–2147 (2013)

Journal of Cellular Biochemistry

Promotion of Mouse Ameloblast Proliferation by Lgr5 Mediated Integrin Signaling

Toshiyuki Yoshida,[1] Takanori Iwata,[1] Terumasa Umemoto,[1] Yoshiko Shiratsuchi,[1] Nobuyuki Kawashima,[2] Toshihiro Sugiyama,[3] Masayuki Yamato,[1] and Teruo Okano[1]*

[1]*Institute of Advanced Biomedical Engineering and Science, Tokyo Women's Medical University, 8-1 Kawada-Cho, Shinjuku-Ku, Tokyo, Japan*

[2]*Pulp Biology and Endodontics, Graduate School of Tokyo Medical and Dental University, 1-5-45 Yushima, Bunkyo-ku, Tokyo, Japan*

[3]*Department of Biochemistry, Akita University School of Medicine, Hondo 1-1-1, Akita, Japan*

ABSTRACT

Rodent incisors grow throughout the animal's lives, and the tooth-forming cells are provided from proximal ends of the incisors where the tooth epithelium forms a stem cell niche called cervical loop. The committing cells in a cervical loop actively begin to proliferate (pre-ameloblasts), and differentiating into ameloblasts. This study showed that the lower incisors of mice null for CD61 (*CD61*$^{-/-}$), also known as integrin β3, were significantly shorter than those of the wild-type mice at 8-week-old. The protein and mRNA expressions levels of Fgfr2, Lgr5, and Notch1, which are known to be involved in pre-ameloblastic cell proliferation and stem cell maintenance, were reduced in the cervical loop of 2-week-old *CD61*$^{-/-}$ mice. The proliferation of pre-ameloblasts was reduced in *CD61*$^{-/-}$ ameloblasts. The siRNA-mediated suppression of *CD61* (siCD61) reduced the proliferation of pre-ameloblastic cell line ALC, and the expression levels of *Lgr5* and *Notch1* were reduced by the transfection with siCD61. The suppression of *Lgr5* by transfection with siLgr5 suppressed the proliferation of the ALC cells. These results suggested that CD61 signaling is required for the proper growth of the cervical loop and for the promotion of the proliferation of pre-ameloblastic cells through Lgr5. J. Cell. Biochem. 114: 2138–2147, 2013.

KEY WORDS: ODONTOGENESIS; INCISOR; CELL PROLIFERATION; HYPOPLASIA; TRANSGENIC MICE; STEM CELL

Unlike other teeth of mammals, incisors of rodents grow continuously, and therefore, dental stem cells are preserved throughout their lives. The stem cells of the incisors reside at their proximal ends where the dental epithelium forms a cervical loop [Harada et al., 1999]. The cervical loop is composed of stellate reticulum (SR) in the core and the basal epithelial layer surrounding the SR region. The basal epithelial layer consists of an inner enamel epithelium (IEE) facing the dental mesenchyme and an outer enamel epithelium (OEE) facing the dental follicle. After being committed, the SR cells enter into the proximal end of IEE and become transit-amplifying (TA) cells, called pre-ameloblasts. Pre-ameloblasts actively proliferate, move distally, and differentiate into ameloblasts [Harada et al., 1999]. The SR cells facing the IEE differentiate into stratum intermedium (SI) cells, which support ameloblast function.

Cell proliferation of mouse incisor cervical loops is controlled by coordination of various signalings including bone morphogenetic proteins (BMPs) [Munne et al., 2009; Wang et al., 2007], fibroblast growth factors (FGFs) [De Moerlooze et al., 2000; Ohuchi et al., 2000; Wang et al., 2007; Klein et al., 2008; Lin et al., 2009; Parsa et al., 2010], Notch [Harada et al., 1999; Tummers and Thesleff, 2003], and several transcription factors [Thomas et al., 1997; Laurikkala et al., 2006]. BMPs expressed in the dental mesenchyme adjacent to the cervical loop suppress the expression of FGFs in the mesenchyme [Wang et al., 2007], and the mesenchymal FGFs maintain the SR cells and promote the proliferation of TA cells. Among those FGFs, Fgf10 is required for cervical loop formation and promotes the proliferation of both TA and SR cells [Harada et al., 1999; Harada et al., 2002]. Fgf10 binds to FGF receptor 2 (Fgfr2) [Ohuchi et al., 2000], and the disruption of Fgfr2 in the dental epithelium causes a strong reduction

This study has no conflict of interest.
Grant sponsor: Ministry of Education, Culture, Sports, Science, and Technology (MEXT), Japan.
*Correspondence to: Teruo Okano, 8-1 Kawada-Cho, Shinjuku-Ku, Tokyo 162-8666, Japan.
E-mail: tokano@abmes.twmu.ac.jp
Manuscript Received: 20 November 2012; Manuscript Accepted: 25 March 2013
Accepted manuscript online in Wiley Online Library (wileyonlinelibrary.com): 4 April 2013
DOI 10.1002/jcb.24564 • © 2013 Wiley Periodicals, Inc.

in the proliferation of dental epithelial cells, resulting in the severe dysplasia of incisors [Lin et al., 2009; Parsa et al., 2010]. TA cells express lunatic fringe, a Notch signaling modulator that is thought to maintain SR cells through Notch1 [Harada et al., 1999], and the disruption of FGF signaling causes the loss of Notch1 expression [Parsa et al., 2010]. In addition to FGF and Notch signaling, the expression of leucine-rich repeat-containing G protein-coupled receptor 5 (Lgr5), a putative epithelial stem cell marker, in cervical loops has been reported [Suomalainen and Thesleff, 2010].

Lgr5, also known as GPR49, is a seven-transmembrane-domain receptor of the R-spondin family, and is known as a one of Wnt target genes [van de Wetering et al., 2002; Van der Flier et al., 2007; Glinka et al., 2011; de Lau et al., 2011]. The expression of Lgr5 is observed in TA cells of several epithelial tissues, including the gastrointestinal tract and hair follicles, and Wnt signaling has been shown to induce the expression of Lgr5 in these tissues [Sato et al., 2006; Barker et al., 2007; Jaks et al., 2008]. Lgr5 positive cells can form a complete epithelial structure of hair follicle, stomach, intestine, and colon in vitro [Sato et al., 2006; Jaks et al., 2008], and can regenerate a colon epithelial structure from a single cell in vivo [Yui et al., 2012]. Thus, Lgr5 is thought to be a stem cell marker for these tissues. In mouse dental epithelium, the expression of Lgr5 is observed in SR cells of embryonic cervical loops of embryonic Day 16 E16) and E18 [Suomalainen and Thesleff, 2010]. However, unlike other tissues, the cervical loops of mouse lower incisors do not express any Wnt ligand, nor do they exhibit canonical Wnt signaling [Suomalainen and Thesleff, 2010].

CD61, also known as integrin β3, is a cell surface molecule belonging to the integrin family. CD61 forms heterodimers with integrin αIIb or αv, and these heterodimers bind to various extracellular matrices [Nieswandt and Watson, 2003]. Previous studies have shown that CD61 signaling is related to various physiological processes including stem-cell maintenance and platelet function [Nieswandt and Watson, 2003; Asselin-Labat et al., 2007; Umemoto et al., 2012]. Mutations in human *CD61* cause Glanzmann thrombasthenia (GT), which is characterized by impaired platelet function [George et al., 1990; Chen et al., 1992]. Because mice lacking *CD61* (*CD61*$^{-/-}$) exhibit abnormalities similar to those of GT patients, *CD61*$^{-/-}$ mice are recognized as an animal model of GT [Hodivala-Dilke et al., 1999]. *CD61*$^{-/-}$ mice also exhibited osteosclerosis and intimal hyperplasia after vascular injury [McHugh et al., 2000; Smyth et al., 2001]. In mouse teeth, CD61 is expressed in the epithelial rests of Malassez (ERM), and is thought to be related to the proliferation of ERM cells during tooth movement and in primary culture [Talic et al., 2004; Nezu et al., 2011]. The present study investigated the teeth of *CD61*$^{-/-}$ mice, and found that lower incisors were shorter than were those of wild-type mice. Although physiological importance of the integrin signaling, the role of integrin signaling for tooth growth is largely unknown. The aim of this study is to investigate the mechanism that integrin signaling control the ameloblast proliferation.

MATERIALS AND METHODS

ANIMALS

C57BL/6-Ly5.2 and C57BL/6-Ly5.1 mice were obtained from Sankyo Labo Service (Tokyo, Japan), and *CD61*$^{-/-}$ mice were obtained from The Jackson Laboratory (Bar Harbor, ME, USA). All of the animal experiments were performed according to the "Guidelines of Tokyo Women's Medical University on Animal Use," the "Principles of Laboratory Animal Care" formulated by the National Society for Medical Research, and the "Guide for the Care and Use of Laboratory Animals" prepared by the Institute of Laboratory Animal Resources and published by the National Institutes of Health (NIH Publication No. 86-23, revised 1985).

X-RAY COMPUTED TOMOGRAPHY (CT)

Skeletal preparations of 8-week-old mouse skulls were prepared as previously described [Mustonen et al., 2003]. Micro-CT images of the mandibular skeletal preparations were obtained using a SkyScan1076 (Skyscan, Kontich, Belgium). The micro-CT images were reconstructed, and scatter and X-ray images were obtained using VG Studio MAX (Nihon Visual Science, Tokyo, Japan). Length of the lower incisor (arch a and b in Fig. 1, Appendix Fig. A1) and mandible (line a–c–d in Fig. 1, Appendix Fig. A1) [Atchley et al., 1985] were measured using Image J (National Institutes of Health, Bethesda, MD, USA).

RNA EXTRACTION, cDNA SYNTHESIS, AND POLYMERASE CHAIN REACTION (PCR)

Cervical loop collection, RNA extraction, cDNA synthesis, and PCR reaction were performed as previously described with some modification [Yoshida et al., 2012]. The following TaqMan probes were used: Amelogenin (Amelx, Mm01166221_m1), E-cadherin (Cdh1, Mm01247357_m1), Bmp4 (Mm00432087_m1), CD61 (Itgb3, Mm00443980_m1), Fgf3 (Mm00433289_m1), Fgf10 (Mm00433275_m1), Fgfr2 (Mm01269930_m1), Lgr5 (Mm00438890_m1), Notch1 (Mm00435249_m1), Rpl4 (Mm01171353_g1), Shh (Mm00436528_m1). Rpl4 were utilized as the internal control genes.

TISSUE PREPARATION, HISTOLOGY, AND IMMUNOHISTOCHEMISTRY

The mouse tissues were fixed with 4% paraformaldehyde, and decalcified with Morse's solution [Morse, 1945; Nakatomi et al., 2006] before embedding in paraffin. Immunostaining was performed as described previously [Laurikkala et al., 2006; Yoshida et al., 2010]. The following primary antibodies were used at the indicated dilutions after antigen retrieval using Antigen Unmasking Solution for 10 min (H3300, Vector Laboratories, Burlingame, CA): Fgfr2 (1:1, ab27481, Abcam, Cambridge, UK), Lgr5 (1:100, ab27526, Abcam), Notch1 (1:100, ab75850, Abcam), phospho-histone H3 (1:800, 06-570, Millipore, Billerica, MA), type IV collagen (1:500, ab19808, Abcam), and E-cadherin (1:200, 13900, Life Technologies, Carlsbad, CA, 1:200).

ALC CELL CULTURE, siRNA TRANSFECTION, AND CELL PROLIFERATION ASSAY

The ALC cells were cultured as previously described [Nakata et al., 2003]. Each siRNA was mixed with Opti-MEM (Life Technologies), and transfected into cells with Lipofectamine RNAiMAX (Life Technologies) using the reverse transfection method according to the manufacturer's protocol. The siRNAs for the following genes were purchased from Life Technologies (Cat. No. 4390771): CD61 (Itgb3, s233398), Notch1 (s70699), and Lgr5

(s65961). Silencer Select Negative Control (siCont, 4390846) was used as a negative control. The cells were plated in 96-well plates at a density of 1.5×10^3 cells/well, and the number of cells was measured at 48 h after transfection using the CellTiter 96 AQueous One Solution Cell Proliferation Assay (Promega, Fitchburg, WI). The absorbance of the medium was normalized to that of the siCont transfected cells.

WESTERN BLOT ANALYSIS

Proteins were extracted using lysis buffer (9803S, Cell Signaling, Beverly, MA) supplemented with a protease inhibitory mix (1:100 80-6501-23, GE Healthcare, Little Chalfont, United Kingdom) and Halt Phosphatase Inhibitor Cocktail (78420, Thermo Fisher Scientific, Waltham, MA). The samples (50 μg per lane) were applied to Nupage Bis–Tris Precast Gels (NP0321BOX, Life Technologies), separated by electrophoresis, and electrotransferred onto nitrocellulose membranes using the iBlot gel transfer system (IB1001, Life Technologies). The membranes were blocked with 5% ECL prime blocking reagent (RPN418, GE Healthcare) in TBST (blocking solution), followed by incubation with antibodies against CD61 (1:1,000, Ab75872, Abcam), the phosphorylated form of JNK1/2/3 (pJNK, 1:1,000, 2155-1, Epitomics, Burlingame, CA), total JNK (1:1,000, #9258, Cell Signaling), pErk1/2 (1:500, V803A, Promega), Erk1/2 (1:1,000, #4695, Cell Signaling) pAkt (1:1,000, 2118-1, Epitomics), Akt (1:1,000, #9272, Cell Signaling), and β-actin (1:1,000, MAB1501R, Millipore), at the indicated concentrations in the blocking solution. The membranes were incubated with peroxidase-linked anti-rabbit or anti-mouse IgG (NA934VS, NA931VS, GE Healthcare, respectively) at 1:20,000 in blocking solution, followed by detection using the ECL Prime Western Blotting Detection Reagent (RPN2232, GE Healthcare). The chemiluminescence was visualized using LAS 4000 UV mini (Fujifilm, Tokyo, Japan), and the intensity of each band was quantified using Multi Gauge (Fujifilm).

DATA ANALYSIS

All of the values are expressed as the mean ± SEM. All of the samples were analyzed using Student's *t*-tests, and values of $P < 0.05$ and $P < 0.01$ were considered statistically significant.

RESULTS

CD61 DEFICIENT MICE EXHIBITED SHORTER LOWER INCISOR

CD61 was expressed in the cervical loop, and the quantitative RT-PCR revealed the lack of wild-type (WT) *CD61* mRNA in CD61 deficient ($CD61^{-/-}$) mice (Appendix Fig. A2). Skeletal preparations of 8-week-old WT and $CD61^{-/-}$ mice revealed that $CD61^{-/-}$ mice had a normal head size, number of teeth, and no abnormalities with respect to size, shape, and color were observed in molars (data not shown). However, the lower incisors of $CD61^{-/-}$ mice lacked pigmentation on their labial surfaces [Yoshida et al., 2012], and the positions of cervical loops were lower than were those in the lower incisors of WT mice (Fig. 1A–F). No significant abnormality was observed in the enamel structure of the $CD61^{-/-}$ lower incisors [Yoshida et al., 2012]. Statistical analysis revealed that relative length of the *CD61* mutant

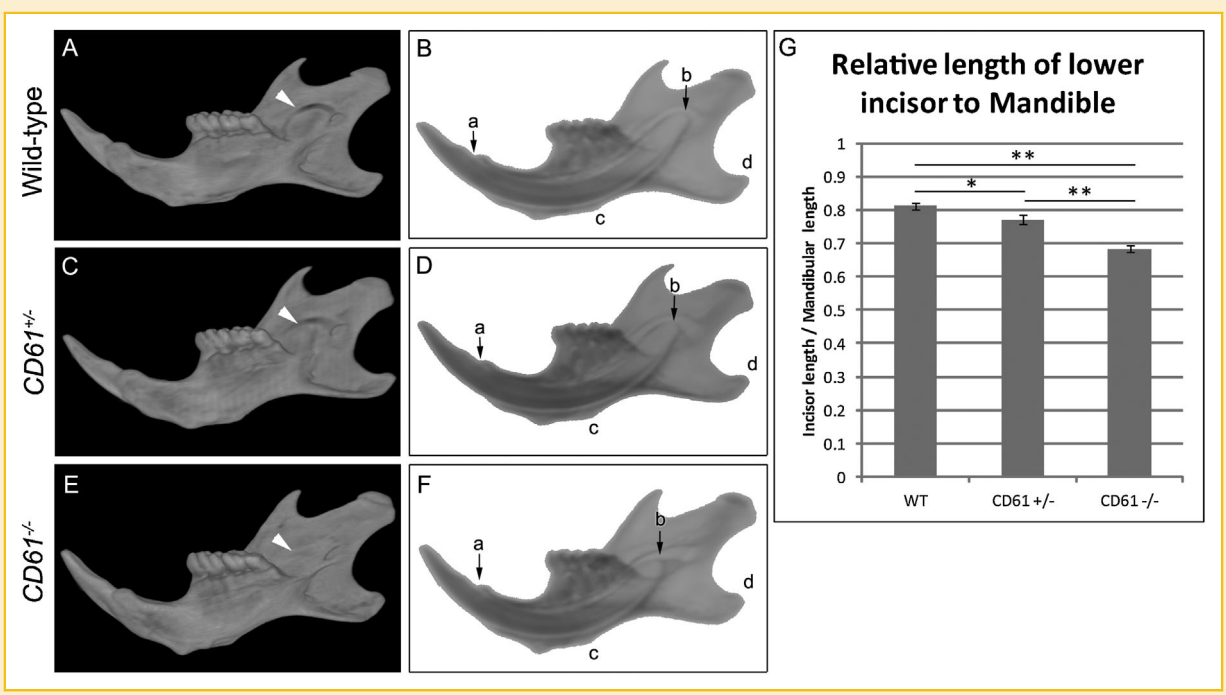

Fig. 1. Micro-CT analysis of the mandibular skeletal preparations. Micro-CT images of the mandibles of 8-week-old WT (A,B), $CD61^{+/-}$ (C,D), and $CD61^{-/-}$ (E,F) mice. A,C,E: Scatter images of the mandibles from the lingual side. A ridge corresponding to the proximal end of the lower incisor is observed in the middle of the mandibular ramus (arrowhead) in WT and $CD61^{+/-}$ mice (A,C), but is barely observed in the $CD61^{-/-}$ mandible (E). B,D,F: X-ray images of the mandibles. G: Relative length of the lower incisors of the WT, $CD61^{+/-}$, and $CD61^{-/-}$ mice. The bars and lines represent the means and SEMs of five samples ($^{*}P < 0.05$, $^{**}P < 0.01$).

lower incisors were significantly shorter than length of the WT lower incisors in genotype dependent manner (Fig. 1G).

Histological analysis confirmed the lower position of cervical loops in *CD61*$^{-/-}$ mice relative to the position in WT mice. The proximal ends of cervical loops were closer to mandibular 2nd molars in *CD61*$^{-/-}$ mice than in WT mice (Fig. 2A,D). Two-week-old *CD61*$^{-/-}$ mice had slightly shorter lower incisors than that in WT mice (Fig. 2G, J). No significant histological abnormality was observed in the cervical loop structure, ameloblasts, and dentin and enamel formation appeared normal in both 2- and 8-week-old mice (Fig. 2A–L).

GROWTH OF CERVICAL LOOP WAS REDUCED IN *CD61*$^{-/-}$ MICE

The expression levels of *Fgfr2*, *Notch1*, and *Lgr5* were reduced in proximal ends of the *CD61*$^{-/-}$ lower incisors compared with that in the WT lower incisors, whereas the expression levels of ameloblastic genes, including *Amelogenin*, *Shh*, and *E-cadherin* and dental mesenchymal genes, including *Fgf3*, *Fgf10*, and *Bmp4*, were comparable (Fig. 3).

In the cervical loops of 2-week-old *CD61*$^{-/-}$ mice, localizations of an adherens junction protein E-cadherin and a basement membrane component type IV collagen were comparable to those in WT mice (Fig. 4A,C, data not shown). The expression of a cell proliferation marker phosphorylated-histone H3 (pHistone H3) exhibited slight, but statistically significant, reduction (Fig. 4B,D,E). In WT mice, Fgfr2 was detected in IEE, OEE, and SR of cervical loops (Fig. 4F). Lgr5 was localized in TA cells of cervical loops (black arrowhead in Fig. 4G), and Notch1 was detected in SI cells (black arrowhead in Fig. 3H). The expression of Fgfr2, Lgr5, and Notch1 were reduced in the cervical loop of 2-week-old *CD61*$^{-/-}$ mice compared with that of WT mice (Fig. 4I, white arrowhead in Fig. 4J,K). Reductions in the expression levels of these genes were also observed at 8 weeks (data not shown).

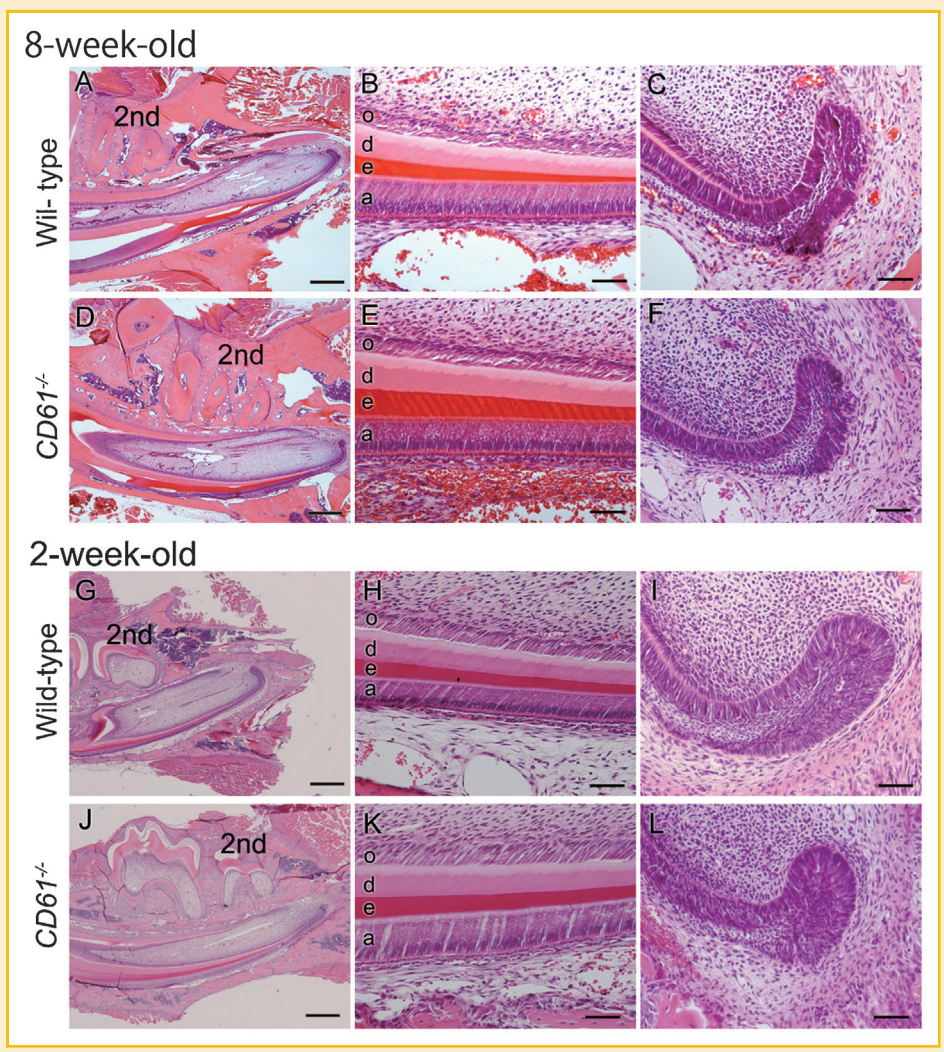

Fig. 2. Histological analysis of WT and *CD61*$^{-/-}$ mandibles. Hematoxylin and eosin staining of 8-week-old (A–F) and 2-week-old (G–L) WT (A–C,G–I) and *CD61*$^{-/-}$ (D–F,J–L) mandibles. A,D,G,J: Lower-magnification image of the lower incisor. The position of the 2nd molar is indicated as "2nd." Scale bars: 250 μm. B,E,H,K: Higher-magnification images of secretary-stage ameloblasts. "a," "e," "d," and "o" indicate ameloblasts, enamel, dentin, and the odontoblast layer, respectively. Scale bars: 50 μm. C,F,I,L: Higher-magnification images of the cervical loop. Scale bars: 50 μm.

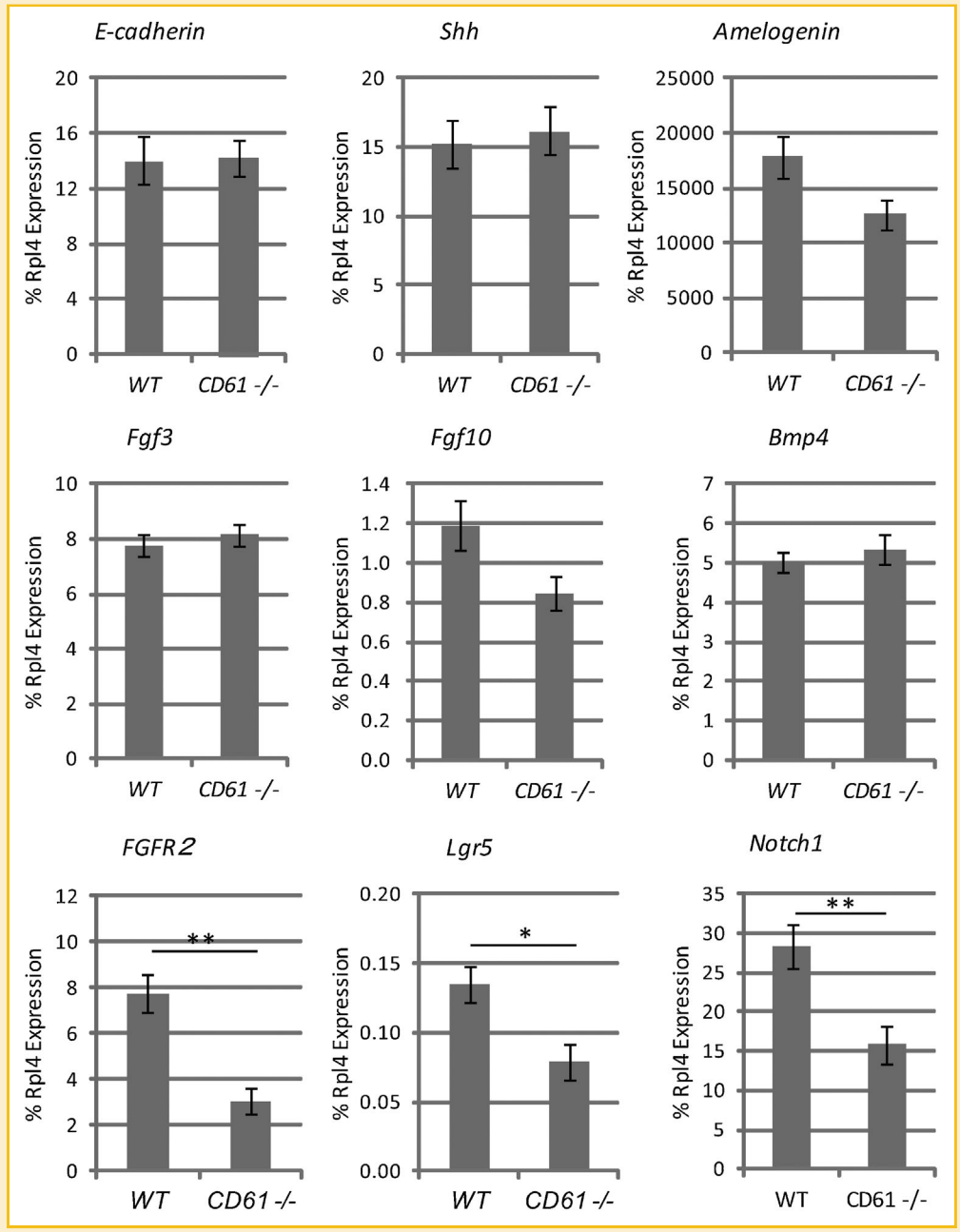

Fig. 3. Gene expression in the WT and *CD61*$^{-/-}$ cervical loops. The expression levels of the indicated genes in the proximal ends of 2-week-old mice lower incisor were analyzed by real-time RT-PCR. The bars and lines represent the means and SEMs of five samples ($^{*}P < 0.05$, $^{**}P < 0.01$).

CD61 SIGNALING PROMOTED THE PROLIFERATION OF AMELOBLASTIC CELL

To investigate the role of CD61 in ameloblast proliferation, the pre-ameloblastic cell line ALC was used for knock-down assays. In ALC cells, transfection with 20 nmol/L or 40 nmol/L siRNA targeting *CD61* (siCD61) significantly reduced both mRNA and protein expressions of CD61 than the cells treated with control siRNA (siCont) at the same concentrations after 96 h (Figs. 5A and 6). The transfection with siCD61 at 40 nmol/L significantly reduced the expression of *Lgr5* and *Notch1* compared with that in same amount of siCont-transfected ALC cells after 96 h (Fig. 5B). In contrast, the transfection with siCD61 did not affect the expression of *Fgfr2* after 96 h (Fig. 5B). The transfection with siCD61 at 20 and 40 nmol/L also resulted in the reduction of the ALC cell number compared with the control cells after 48 h (Fig. 5C). At that time point, the expression of *Lgr5* already exhibited a significant reduction by transfection with siCD61 at 40 nmol/L compared with siCont at same amount, whereas the expression of *Notch1* was comparable to that in the siCont-transfected cells (Fig. 5D).

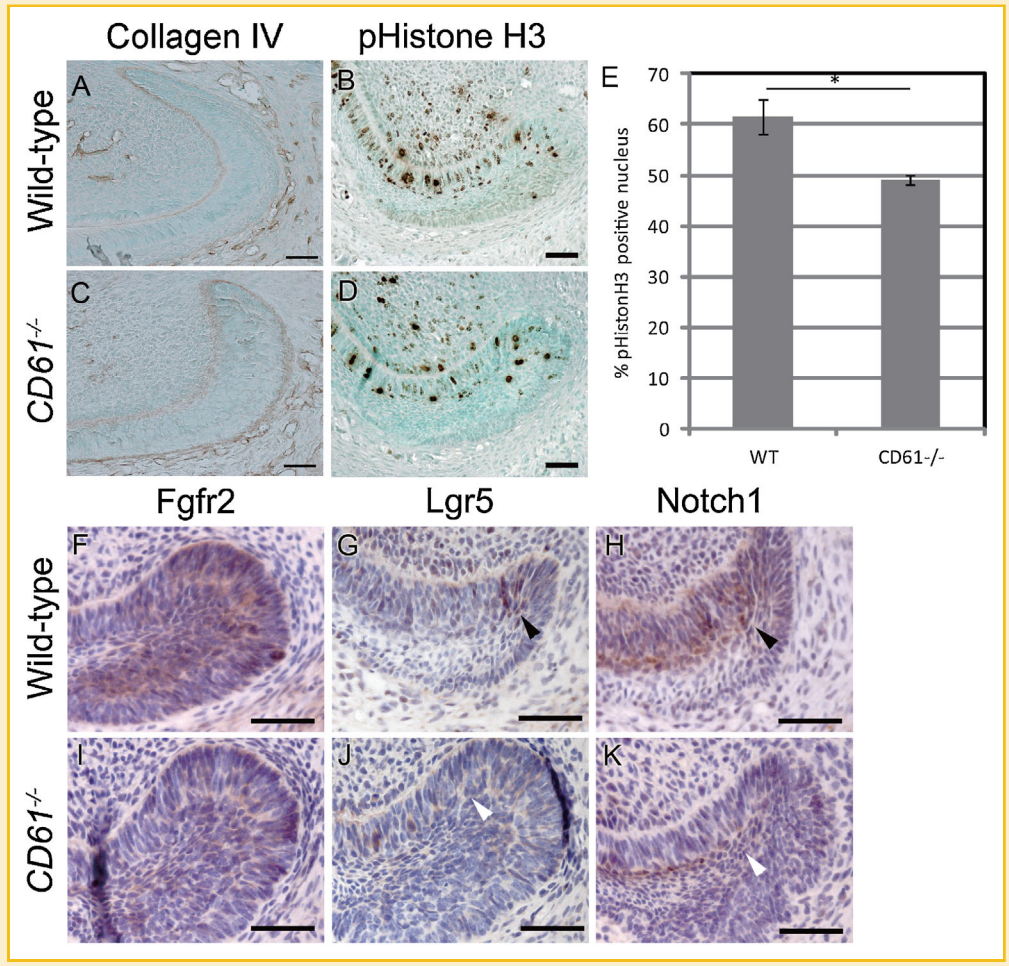

Fig. 4. Protein localization in the WT and *CD61*$^{-/-}$ cervical loops. Immunostaining analyses of collagen IV (A,C), pHistone H3 (B,D), Fgfr2 (F,I), Lgr5 (G,J), and Notch1 (H,K), and in the cervical loops of 2-week-old WT (A,B,F–H) and *CD61*$^{-/-}$ mice (C,D,I–K). Scale bars: 50 μm. E: Quantification of % pHistone H3 positive nucleus in TA region The bars and lines represent the means and SEMs of six samples ($^{*}P < 0.05$).

The transfections with siLgr5 and siNotch1 significantly reduced the expression of *Lgr5* and *Notch1* compared with that in siCont-transfected cells after 96 h (Fig. 5E,F). The number of siLgr5-transfected cells was significantly reduced compared with that of siCont-transfected cells after 48 h, whereas transfection with siNotch1 had no effect on the ALC cell number (Fig. 5G).

The transfection of siCD61 resulted in the reduction of pJNK 1/2/3, and slight reduction of pAkt whereas the total amount of each protein and amount of pErk 1/2 was not affected compared with the transfection of siCont in ALC cells (Fig. 6, data not shown).

DISCUSSION

This study found that a lack of CD61 in mice caused a shortening of the lower incisors from 2 weeks of age and that the severity was dependent on the genotype. Previous studies have reported the expression of CD61 in ERM, but the role of CD61 signaling in tooth development is largely unknown. The short lower incisor phenotype is also observed in mice expressing dominant-negative Fgfr2, and these mice show a severe proliferation defect in the dental epithelium [Parsa et al., 2010]. Thus, the short lower incisors observed in *CD61*$^{-/-}$ mice was hypothesized to be caused by the reduced proliferation of ameloblasts.

Previous studies have reported that FGF and Notch signaling promote the proliferation and stem cell maintenance of cervical loop cells [Harada et al., 1999, 2002; Klein et al., 2008; Lin et al., 2009; Parsa et al., 2010], and the expression of a epithelial TA cell marker Lgr5 in cervical loops has also been reported. Although the previous study showed the expression of Lgr5 in SR region [Suomalainen and Thesleff, 2010], but the expression of Lgr5 was detected in TA region in this study. This may reflect the stage difference between these two studies (E18, and 2-week-old, respectively). Both the mRNA and protein expression levels of these genes were reduced in the cervical loop of *CD61*$^{-/-}$ mice. Consistent to these results, the proliferation of TA cells were slightly reduced in *CD61*$^{-/-}$ mice compared with controls, and this was thought to be the cause of shorter lower incisor.

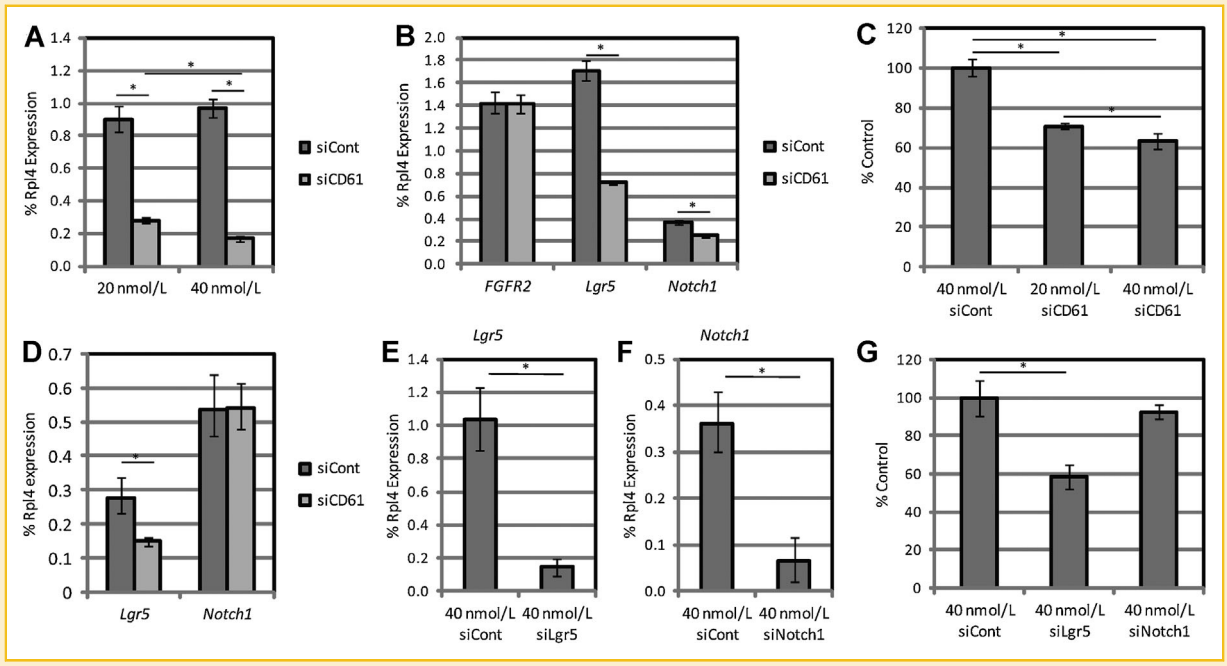

Fig. 5. Effect of siRNA transfection on ALC cells. The bars and lines represent the means and SEMs of three samples (* $P < 0.01$). A: Real-time RT-PCR analyses of *CD61* expression at 96 h after the transfection with siCD61 or siCont. B: Real-time RT-PCR analyses of *Fgfr2*, *Lgr5*, and *Notch1* at 96 h after transfection with siCD61 or siCont. C: The number of ALC cells at 48 h after transfection with siCD61 or siCont at 20 or 40 nmol/L. D: Real-time RT-PCR analyses of *Lgr5* and *Notch1* at 48 h after transfection with siCD61 or siCont. E: Real-time RT-PCR analyses of *Lgr5* expression at 96 h after transfection with siLgr5 or siCont. F: Real-time RT-PCR analyses of *Notch1* expression at 96 h after transfection with siNotch1 or siCont. G: The number of ALC cells at 48 h after transfection with 40 nmol/L of siLgr5, siNotch1, or siCont.

However, these abnormalities were much milder than those due to the disruption of FGF signaling, which led to the loss of incisors [Lin et al., 2009; Parsa et al., 2010]. This result suggested that the residual expression of these genes was sufficient to promote the proliferation and differentiation of cervical loop cells, and that CD61 signaling may play a supportive role in the growth of cervical loop.

The mouse pre-ameloblastic cell line ALC was utilized in this study to investigate the role of CD61 signaling in the proliferation of cervical loop cells in detail. ALC cells are derived from mouse dental epithelial cells, and express enamel-related proteins, including amelogenin and enamelin [Nakata et al., 2003; Takahashi et al., 2007]. Thus, ALC cells have been used to investigate the

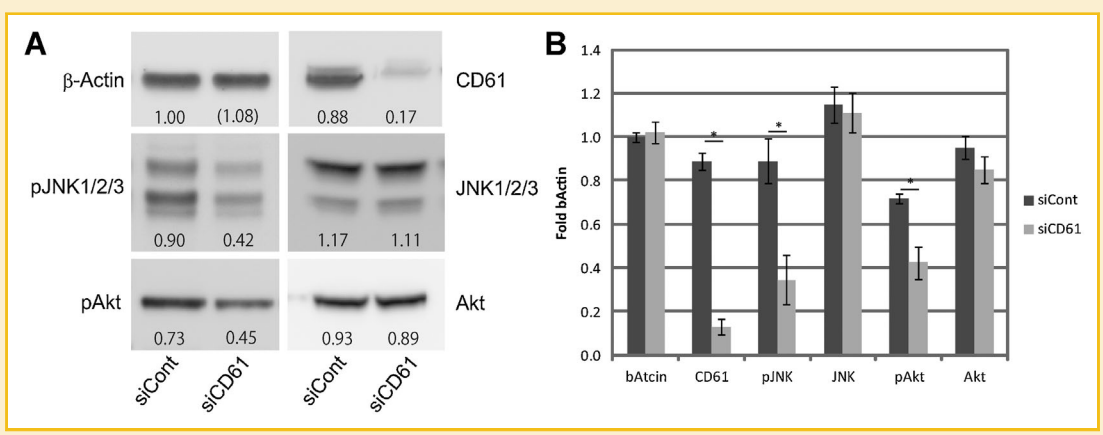

Fig. 6. A: Western blot analysis of CD61 and phosphorylation of proteins involved in integrin signaling in ALC cells. The Western blot analysis of CD61, phosphorylated and total protein of Jnk1/2/3 and Akt was performed using the protein extracted from ALC cells at 96 h after the transfection with siCont or siCD61. The numbers below the bands indicate the relative intensities of the bands relative to the β-actin band. B: Densitometric analysis of A. The bars and lines indicate the means and SEMs of four samples (* $P < 0.01$).

properties of ameloblasts in vitro [Tsuchiya et al., 2009; Lee et al., 2010]. The TA cells (pre-ameloblasts) of *CD61*$^{-/-}$ exhibited the reduced proliferation and expression of proliferation related genes, and ALC cells expressed *Fgfr2*, *Lgr5*, *Notch1* as observed in TA cells of cervical loop. Thus, the ALC cells were suitable for investigating the role of CD61 signaling in the present study. Transfection with siCD61 efficiently suppressed both the mRNA and protein expression of CD61, and the suppression of *CD61* resulted in the reduction of ALC cell proliferation. Inconsistent with the results of immunohistochemical and gene expression assays of *CD61*$^{-/-}$ in cervical loops, the suppression of *CD61* resulted in no effect on the expression of *Fgfr2*. Although the expression of *Notch1* exhibited only a slight reduction at 96 h after transfection with siCD61, transfection with siNotch1 had no effect on ALC proliferation. These results suggested that *Fgfr2* and *Notch1* were not direct downstream of CD61 signaling pathway. Although the reductions of Fgfr2 and Notch1 might be involved in the development of short lower incisors in *CD61*$^{-/-}$ mice, the reduction of Fgfr2 and Notch1 expressions might be a secondary effects of CD61 deficiency. In contrast, the expression of *Lgr5* was severely disrupted by the siCD61 transfection, and siLgr5 suppressed the proliferation of the ALC cells, consistent with the results of previous studies showing that Lgr5-positive cells actively proliferate [Barker et al., 2007; Jaks et al., 2008; Sato et al., 2009]. The results of Western blot analysis of phosphorylated proteins known to mediate integrin signaling suggested that CD61 signaling was predominantly based on the JNK and/or Akt pathways, and not the Erk pathway. These results suggested that CD61 signaling promoted Lgr5 expression, which positively regulated the proliferation of the ALC cells.

Although previous studies have reported the expression of *Lgr5* in lizard dental epithelial stem cells and the mouse cervical loop, the signal inducing *Lgr5* expression in the mouse dental epithelium is not clear [Handrigan et al., 2010; Suomalainen and Thesleff, 2010]. In the present study, both in vivo and in vitro results suggested that the CD61 signaling up-regulated Lgr5 expression in pre-ameloblastic cells. Correlations between integrin and Lgr5 are also observed in hair follicle and mammary epithelial cells. In hair follicle stem cells, Lgr5-expressing cells also express integrin α6 [Jaks et al., 2008], and mammary progenitor cells express both CD61 and Lgr5 [Asselin-Labat et al., 2007; Barker et al., 2007]. This study suggested the relationship between CD61 and Lgr5, although the underlying mechanisms remain to be elucidated. In conclusion, CD61 signaling promoted the proliferation of pre-ameloblastic cells through Lgr5, and was partially responsible for the growth of the cervical loop of mouse lower incisors.

ACKNOWLEDGEMENTS

Authors thank Norio Ueno for language editing and support in preparation of the manuscript. This study was supported by the Formation of Innovation Center for Fusion of Advanced Technologies in the Special Coordination Funds for Promoting Science and Technology "Cell Sheet Tissue Engineering Center (CSTEC)," the Formation of Innovation Center for Fusion of Advanced Technologies and the Special Coordination Funds for Promoting Science and Technology from the Ministry of Education, Culture, Sports, Science, and Technology (MEXT), Japan.

REFERENCES

Asselin-Labat ML, Sutherland KD, Barker H, Thomas R, Shackleton M, Forrest NC, Hartley L, Robb L, Grosveld FG, van der Wees J, Lindeman GJ, Visvader JE. 2007. Gata-3 is an essential regulator of mammary-gland morphogenesis and luminal-cell differentiation. Nat Cell Biol 9:201–209.

Atchley WR, Plummer AA, Riska B. 1985. Genetic analysis of size-scaling patterns in the mouse mandible. Genetics 111:579–595.

Barker N, van Es JH, Kuipers J, Kujala P, van den Born M, Cozijnsen M, Haegebarth A, Korving J, Begthel H, Peters PJ, Clevers H. 2007. Identification of stem cells in small intestine and colon by marker gene Lgr5. Nature 449:1003–1007.

Boell L, Tautz D, 2011. Micro-evolutionary divergence patterns of mandible shapes in wild house mouse (Mus musculus) populations. BMC Evol Biol 11:306.

Chen YP, Djaffar I, Pidard D, Steiner B, Cieutat AM, Caen JP, Rosa JP. 1992. Ser-752 → Pro mutation in the cytoplasmic domain of integrin beta 3 subunit and defective activation of platelet integrin alpha IIb beta 3 (glycoprotein IIb-IIIa) in a variant of Glanzmann thrombasthenia. Proc Natl Acad Sci USA 89:10169–10173.

de Lau W, Barker N, Low TY, Koo BK, Li VS, Teunissen H, Kujala P, Haegebarth A, Peters PJ, van de Wetering M, Stange DE, van Es JE, Guardavaccaro D, Schasfoort RB, Mohri Y, Nishimori K, Mohammed S, Heck AJ, Clevers H. 2011. Lgr5 homologues associate with Wnt receptors and mediate R-spondin signalling. Nature 476:293–297.

De Moerlooze L, Spencer-Dene B, Revest JM, Hajihosseini M, Rosewell I, Dickson C. 2000. An important role for the IIIb isoform of fibroblast growth factor receptor 2 (FGFR2) in mesenchymal–epithelial signalling during mouse organogenesis. Development 127:483–492.

George JN, Caen JP, Nurden AT. 1990. Glanzmann's thrombasthenia: The spectrum of clinical disease. Blood 75:1383–1395.

Glinka A, Dolde C, Kirsch N, Huang YL, Kazanskaya O, Ingelfinger D, Boutros M, Cruciat CM, Niehrs C. 2011. LGR4 and LGR5 are R-spondin receptors mediating Wnt/beta-catenin and Wnt/PCP signalling. EMBO Rep 12:1055–1061.

Handrigan GR, Leung KJ, Richman JM. 2010. Identification of putative dental epithelial stem cells in a lizard with life-long tooth replacement. Development 137:3545–3549.

Harada H, Kettunen P, Jung HS, Mustonen T, Wang YA, Thesleff I. 1999. Localization of putative stem cells in dental epithelium and their association with Notch and FGF signaling. J Cell Biol 147:105–120.

Harada H, Toyono T, Toyoshima K, Yamasaki M, Itoh N, Kato S, Sekine K, Ohuchi H. 2002. FGF10 maintains stem cell compartment in developing mouse incisors. Development 129:1533–1541.

Hodivala-Dilke KM, McHugh KP, Tsakiris DA, Rayburn H, Crowley D, Ullman-Cullere M, Ross FP, Coller BS, Teitelbaum S, Hynes RO. 1999. Beta3-integrin-deficient mice are a model for Glanzmann thrombasthenia showing placental defects and reduced survival. J Clin Invest 103:229–238.

Jaks V, Barker N, Kasper M, van Es JH, Snippert HJ, Clevers H, Toftgard R. 2008. Lgr5 marks cycling, yet long-lived, hair follicle stem cells. Nat Genet 40:1291–1299.

Klein OD, Lyons DB, Balooch G, Marshall GW, Basson MA, Peterka M, Boran T, Peterkova R, Martin GR. 2008. An FGF signaling loop sustains the generation of differentiated progeny from stem cells in mouse incisors. Development 135:377–385.

Laurikkala J, Mikkola ML, James M, Tummers M, Mills AA, Thesleff I. 2006. p63 regulates multiple signalling pathways required for ectodermal organogenesis and differentiation. Development 133:1553–1563.

Lee HK, Lee DS, Ryoo HM, Park JT, Park SJ, Bae HS, Cho MI, Park JC. 2010. The odontogenic ameloblast-associated protein (ODAM) cooperates with RUNX2 and modulates enamel mineralization via regulation of MMP-20. J Cell Biochem 111:755–767.

Lin Y, Cheng YS, Qin C, Lin C, D'Souza R, Wang F. 2009. FGFR2 in the dental epithelium is essential for development and maintenance of the maxillary cervical loop, a stem cell niche in mouse incisors. Dev Dyn 238: 324–330.

McHugh KP, Hodivala-Dilke K, Zheng MH, Namba N, Lam J, Novack D, Feng X, Ross FP, Hynes RO, Teitelbaum SL. 2000. Mice lacking beta3 integrins are osteosclerotic because of dysfunctional osteoclasts. J Clin Invest 105:433–440.

Morse A. 1945. Formic acid–sodium citrate decalcification and butyl alcohol dehydration of teeth and bones for sectioning in paraffin. J Dent Res 24:143–153.

Munne PM, Tummers M, Jarvinen E, Thesleff I, Jernvall J. 2009. Tinkering with the inductive mesenchyme: Sostdc1 uncovers the role of dental mesenchyme in limiting tooth induction. Development 136:393–402.

Mustonen T, Pispa J, Mikkola ML, Pummila M, Kangas AT, Pakkasjarvi L, Jaatinen R, Thesleff I. 2003. Stimulation of ectodermal organ development by ectodysplasin-A1. Dev Biol 259:123–136.

Nakata A, Kameda T, Nagai H, Ikegami K, Duan Y, Terada K, Sugiyama T. 2003. Establishment and characterization of a spontaneously immortalized mouse ameloblast-lineage cell line. Biochem Biophys Res Commun 308: 834–839.

Nakatomi M, Morita I, Eto K, Ota MS. 2006. Sonic hedgehog signaling is important in tooth root development. J Dent Res 85:427–431.

Nezu T, Matsuyoshi N, Nishii Y, Sueishi K, Inoue T. 2011. The effect of aging on the functions of epithelial rest cells of Malassez in vitro: immunofluorescence, DNA microarray and RT-PCR analyses. Oral Med Pathol 15:101–106.

Nieswandt B, Watson SP. 2003. Platelet–collagen interaction: Is GPVI the central receptor? Blood 102:449–461.

Ohuchi H, Hori Y, Yamasaki M, Harada H, Sekine K, Kato S, Itoh N. 2000. FGF10 acts as a major ligand for FGF receptor 2 IIIb in mouse multi-organ development. Biochem Biophys Res Commun 277:643–649.

Parsa S, Kuremoto K, Seidel K, Tabatabai R, Mackenzie B, Yamaza T, Akiyama K, Branch J, Koh CJ, Al Alam D, Klein OD, Bellusci S. 2010. Signaling by FGFR2b controls the regenerative capacity of adult mouse incisors. Development 137:3743–3752.

Sato T, Fujita N, Yamada A, Ooshio T, Okamoto R, Irie K, Takai Y. 2006. Regulation of the assembly and adhesion activity of E-cadherin by nectin and afadin for the formation of adherens junctions in Madin–Darby canine kidney cells. J Biol Chem 281:5288–5299.

Sato T, Vries RG, Snippert HJ, van de Wetering M, Barker N, Stange DE, van Es JH, Abo A, Kujala P, Peters PJ, Clevers H. 2009. Single Lgr5 stem cells build crypt-villus structures in vitro without a mesenchymal niche. Nature 459:262–265.

Smyth SS, Reis ED, Zhang W, Fallon JT, Gordon RE, Coller BS. 2001. Beta (3)-integrin-deficient mice but not P-selectin-deficient mice develop intimal hyperplasia after vascular injury: Correlation with leukocyte recruitment to adherent platelets 1 hour after injury. Circulation 103:2501–2507.

Suomalainen M, Thesleff I. 2010. Patterns of Wnt pathway activity in the mouse incisor indicate absence of Wnt/beta-catenin signaling in the epithelial stem cells. Dev Dyn 239:364–372.

Takahashi S, Kawashima N, Sakamoto K, Nakata A, Kameda T, Sugiyama T, Katsube K, Suda H. 2007. Differentiation of an ameloblast-lineage cell line (ALC) is induced by Sonic hedgehog signaling. Biochem Biophys Res Commun 353:405–411.

Talic N, Evans CA, Daniel JC, George A, Zaki AM. 2004. Immunohistochemical localization of alphavbeta3 integrin receptor during experimental tooth movement. Am J Orthod Dentofacial Orthop 125:178–184.

Thomas BL, Tucker AS, Qui M, Ferguson CA, Hardcastle Z, Rubenstein JL, Sharpe PT. 1997. Role of Dlx-1 and Dlx-2 genes in patterning of the murine dentition. Development 124:4811–4818.

Tsuchiya M, Sharma R, Tye CE, Sugiyama T, Bartlett JD. 2009. Transforming growth factor-b1 expression is up-regulated in maturation-stage enamel organ and may induce ameloblast apoptosis. Eur J Oral Sci 117:105–112.

Tummers M, Thesleff I. 2003. Root or crown: A developmental choice orchestrated by the differential regulation of the epithelial stem cell niche in the tooth of two rodent species. Development 130:1049–1057.

Umemoto T, Yamato M, Ishihara J, Shiratsuchi Y, Utsumi M, Morita Y, Tsukui H, Terasawa M, Shibata T, Nishida K, Kobayashi Y, Petrich BG, Nakauchi H, Eto K, Okano T. 2012. Integrin-alphavbeta3 regulates thrombopoietin-mediated maintenance of hematopoietic stem cells. Blood 119:83–94.

van de Wetering M, Sancho E, Verweij C, de Lau W, Oving I, Hurlstone A, van der Horn K, Batlle E, Coudreuse D, Haramis AP, Tjon-Pon-Fong M, Moerer P, van den Born M, Soete G, Pals S, Eilers M, Medema R, Clevers H. 2002. The beta-catenin/TCF-4 complex imposes a crypt progenitor phenotype on colorectal cancer cells. Cell 111:241–250.

Van der Flier LG, Sabates-Bellver J, Oving I, Haegebarth A, De Palo M, Anti M, Van Gijn ME, Suijkerbuijk S, Van de Wetering M, Marra G, Clevers H. 2007. The intestinal Wnt/TCF signature. Gastroenterology 132:628–632.

Wang XP, Suomalainen M, Felszeghy S, Zelarayan LC, Alonso MT, Plikus MV, Maas RL, Chuong CM, Schimmang T, Thesleff I. 2007. An integrated gene regulatory network controls stem cell proliferation in teeth. PLoS Biol 5:e159.

Yoshida T, Miyoshi J, Takai Y, Thesleff I. 2010. Cooperation of nectin-1 and nectin-3 is required for normal ameloblast function and crown shape development in mouse teeth. Dev Dyn 239:2558–2569.

Yoshida T, Kumashiro Y, Iwata T, Ishihara J, Umemoto T, Shiratsuchi Y, Kawashima N, Sugiyama T, Yamato M, Okano T. 2012. Requirement of integrin beta3 for iron transportation during enamel formation. J Dent Res 91:1154–1159.

Yui S, Nakamura T, Sato T, Nemoto Y, Mizutani T, Zheng X, Ichinose S, Nagaishi T, Okamoto R, Tsuchiya K, Clevers H, Watanabe M. 2012. Functional engraftment of colon epithelium expanded in vitro from a single adult Lgr5(+) stem cell. Nat Med 18:618–623.

APPENDIX A

FIGURES A1 AND A2

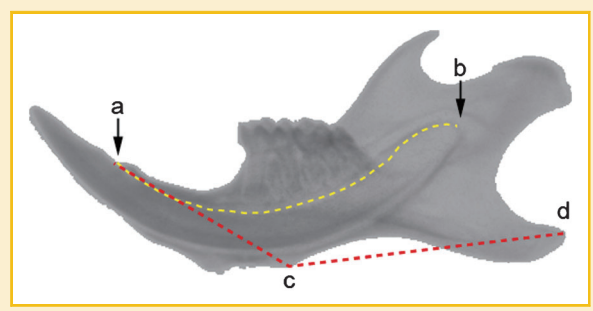

Fig. A1. The length of mandible was calculated by the sum of anterior (a–c) and posterior (c–d) length of mandible (red line) [Atchley et al., 1985]. The length of lower incisor was represented by the length of arch a–b (yellow line). Length of each line was measured using Image J. a: anterior terminus of bone dorsal of the incisor, b: proximal end of lower incisor, c: posterior margin of muscle insertion area on ventral side of incisor ramus, d: posterodorsal tip of processus angularis [Boell and Tautz, 2011].

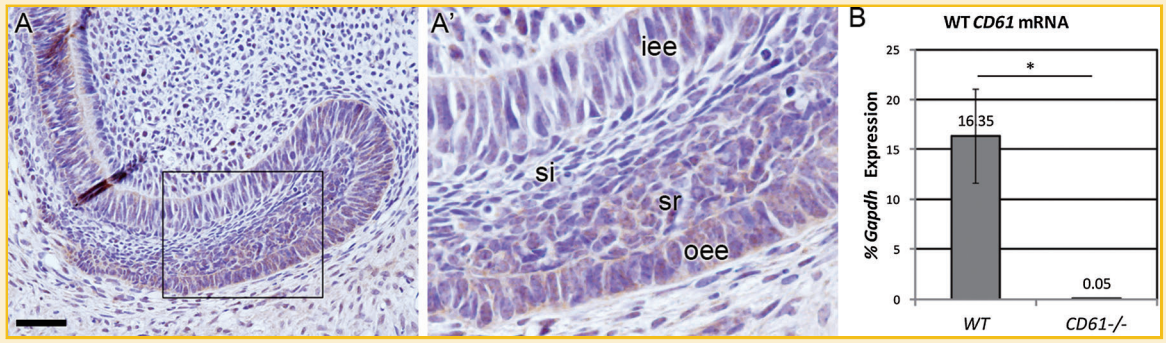

Fig. A2. Expression of CD61 in the cervical loops of 2-week-old mice. A: Immunohistochemical analysis of CD61 using antibody against CD61 (1:200, ab47584, Abcam) in the cervical loops of 2-week-old mice. si, sr, iee, oee, and si indicate the stratum intermedium, stellate reticulum, inner and outer enamel epithelium, respectively. The box in A indicates the area magnified in A′. Scale bar: 50 μm. B: WT *CD61* mRNA expression in the cervical loops of 2-week-old mice was analyzed by real-time RT-PCR. SYBR Green-based quantitative RT-PCR for exon 1, which was removed in the mutant CD61 allele [Hodivala-Dilke et al., 1999], using following primers; CD61 (forward: cctccgcaggaaaagcag, reverse: agagcggcccagagttgt), GAPDH (forward: accacagtccatgccatcac, reverse: tccaccaccctgttgctgta). The bars and lines represent the means and SEMs of three samples ($^{*}P < 0.01$).